

Theoretical and Experimental Performance Analysis on Error-bounded Quantum Search Process*

FU Jianling · XU Ming · QIAN Haifeng · LI Zhi-Bin

DOI:

Received: February 20 2024 / Revised: June 8 2024

©The Editorial Office of JSSC & Springer-Verlag GmbH Germany 2021

Abstract Grover’s algorithm (a. k. a. quantum search process) is one of the most distinguished quantum algorithms, addressing the fundamental problem — how to find goal records from a huge but unstructured database efficiently. It can achieve a relatively optimal success probability after a few Grover iterations for amplitude amplification, which results in a quadratic speed-up in the whole process in terms of the size of database. However, it does not guarantee to achieve that probability within a user-specified error tolerance. So error-bounded quantum search process comes into being. The existing methods introduce extra qubits to meet that tolerance, or exploit high-precision (nonbasic) gates, each of which would be converted to a sequence of basic gates and thus costs much more computational units. In this paper, we employ the strategy of performing more Grover iterations expecting one of a series of local optima to meet the tolerance. To ensure it work rigorously, we identify and exclude three exceptional instances by algebraic number theory, which is reported for the first time. Then we analyze the theoretical complexity of the employed method. It turns out to be in time exponential in the encoding size of the tolerance using basic gates, comparable to the existing method’s, while extra space consumption is saved. The experimental performance is validated by extensive examples from real-world data sets ASRS and public Amazon review.

Keywords Grover’s algorithm, amplitude amplification, performance evaluation, fault tolerance

FU Jianling · LI Zhi-Bin

Shanghai Institute for AI Education, East China Normal University, Shanghai 200062, China.

Email: scsse_fjl2015@126.com, lizb@cs.ecnu.edu.cn

XU Ming · QIAN Haifeng

Shanghai Key Laboratory of Trustworthy Computing, East China Normal University, Shanghai 200062, China.

Email: mxu@cs.ecnu.edu.cn, hfqian@cs.ecnu.edu.cn

*This research was supported by National Natural Science Foundation of China under Grant Nos. 12271172 & 11871221, the National Key R&D Program of China under Grant No. 2018YFA0306704, the Fundamental Research Funds for the Central Universities under Grant No. 2021JQRH014, and the “Digital Silk Road” Shanghai International Joint Lab of Trustworthy Intelligent Software under Grant No. 22510750100.

◇

1 Introduction

Over the past few decades, quantum computing has been advancing rapidly to enable the application of quantum mechanics to computer science for exploring problem-solving capabilities beyond classical computers. As one of the most distinguished quantum algorithms known so far, Grover's algorithm [11] (a.k.a. quantum search process) aims to find one goal record from a huge but unstructured database with relatively optimal probability, which demonstrates the quadratic speed-up surpassing any existing classical algorithm. Exploiting by this advantage, more and more quantum search-based algorithms are being developed and used in a wide range of real-world applications, such as quantum walks [8], equation-solving [7, 9, 14], weight decision problems [15], and hence being expected to demonstrate potential in optimization issues [27].

Speaking technically, Grover's algorithm performs a simply-precomputed times T of the so-called Grover iterations (to be recalled in Section 2) for amplitude amplification. When the number of goal records is greater than one, the algorithm still works [1, 5, 16]. We focus on the multiple-goal situation in this paper to achieve error-bounded analysis. Specifically, we let

- N be the number of all records, and
- M be the number of goal records,

both of which are supposed to be known in advance. By geometric viewpoint, each Grover iteration makes a rotation of angle $\theta = 2 \arcsin(M/N)$ from the initial state $\frac{\theta}{2}$ toward the ideal state $\frac{\pi}{2}$ that means a successful search, i.e. success probability being 1. Then T is preferably chosen to be $\lfloor \frac{\pi}{4} \cdot \sqrt{N/M} \rfloor$ to achieve a relative optimum. Here the relative optimum means that $T \pm i$ times of Grover iterations yield no more success probability than T times do, for a small integer perturbation i . However, it does not guarantee to achieve the success probability $1 - \varepsilon$ for an appointed error tolerance ε . This motivates us to study the error-bounded quantum search process.

For that problem, people have proposed several methods in the beginning of the current century. One of them is to simply narrow the rotation angle of each Grover iteration by inserting plain records into the database (to be described in Section 3). The time complexity of the method is exponential in the encoding size $\|\varepsilon\| = \lceil \log_2(1/\varepsilon) \rceil$ of the given tolerance ε , while inserting plain records requires extra space cost. Hence it will be served as the counterpart of the present work. On the other hand, [5, 16, 20] proposed different strategies to achieve the success probability 1 theoretically. In these methods, the states after Grover iterations correspond to unit vectors in the Bloch sphere, with which Grover iteration corresponds to the composite of two rotations through some appropriate axis of angle π , while the composite of those rotations of angle $\alpha < \pi$ yields a fractional times of Grover iteration, so that it could hit the goal state $\frac{\pi}{2}$ certainly. These elaborated methods need the ability of preparing the rotation gates of some nontypical angle $\alpha \notin \mathbb{Q} \cdot \pi$ that are nonbasic gates and cannot be really implemented in practice. That is why these methods are said to be *theoretical*, not *algorithmic*. However, thanks to the universality of Hadamard, phase, $\frac{\pi}{8}$ and CNOT gates [22, Subsection 4.5.3], those rotation gates could be approximated to any precision, which is also led to an error-bounded quantum search

process. The complexity of the approximation process will be discussed in Section 7, along with our performance analysis. Later on, Grover’s-like methods have been widely developed, e.g., in the subsequent work [17] and the very recent one [19].

Besides, there were a series of work [4, 6, 12, 26] attempting to increase the success probability with monotonically convergent iterations regardless of the prior knowledge about the ratio M/N . For example, a critical paper [12] was realized by fixing the rotation of angle $\frac{\pi}{3}$ during each Grover iteration. In order to apply quantum search in more realistic environment with noise, another work line [2, 24] was studying the fault-tolerance of Grover’s algorithm, i.e., the query transformation in search steps may fail with a fixed probability. Nevertheless, none guarantees that the failure probability of searching could meet the given error bound ε .

In this paper, we study an error-bounded quantum search process that uses *basic* gates only and does *not* require any extra working qubits to achieve the desired amount of success probability. Its strategy is rather easy to follow: Just performing more Grover iterations to expect that one of the reachable states meets the success probability $1 - \varepsilon$. It suffices to give an explicit upper bound of the number of Grover iterations, within which the desired state is hit with a satisfactory probability. First, the realizability of the strategy should be rigorously guaranteed, i.e., the success probability $1 - \varepsilon$ being really achievable even if we do not know how many iterations are sufficient. We resort to the algebraic number theory to settle it. The result reveals there are only three exceptional instances that invalidate the strategy, which can be easily identified and excluded. We then employ the strategy with ease to achieve the success probability $1 - \varepsilon$. The algorithmic complexity turns out to be in time exponential in the encoding size $\|\varepsilon\|$, which is similar to the aforementioned existing method’s while extra space consumption is saved!

We experiment our strategy on real-world data sets — Aviation Safety Reporting System (ASRS) and public Amazon review. Extensive examples from them further show that the upper bound of the required times is not tight, entailing the method is promisingly efficient in practice. The contributions of the present paper are triple-fold:

1. Three exceptional instances are recognized for the strategy of performing more Grover iterations, which is reported for the first time as far as we know.
2. The theoretical performance of that strategy is shown in exponential time without extra space consumption.
3. Experimenting on ASRS and public Amazon review databases validates the performance.

Organization The rest of the paper is organized as follows. We recall basic notations from quantum computing and Grover’s algorithm in Section 2, which will motivate the error-bounded quantum search process. To this end, Section 3 introduces an existing method together with performance analysis. Then we raise another as comparison, whose theoretical guarantee is given in Section 4 and performance is analyzed in Section 5. Experimentation is delivered in Section 6. Finally this paper is concluded in Section 7.

2 Preliminaries

First of all, we recall some basic notions and notations from quantum computing [22], and describe the rationale of Grover's algorithm [11].

2.1 Dirac notations

Classical single bits are simply represented by either 0 or 1. In quantum world, they are quantitized as the unit column vectors $|0\rangle = [1, 0]^T$ and $|1\rangle = [0, 1]^T$ in the two-dimensional Hilbert space \mathbb{H} that is a vector space over complex numbers \mathbb{C} equipped with some inner product $\langle \cdot | \cdot \rangle$, satisfying:

- $\langle \Psi | \Psi \rangle = \langle \Psi | \Psi \rangle \geq 0$ for any (unnecessarily unit) vector $|\Psi\rangle$, where the equality holds if and only if $|\Psi\rangle = 0$;
- $\langle \Psi_1 | \Psi_2 \rangle = \langle \Psi_2 | \Psi_1 \rangle^*$ for any vectors $|\Psi_1\rangle$ and $|\Psi_2\rangle$, where $*$ denotes complex conjugate;
- $\langle \Psi | c_1 \Psi_1 + c_2 \Psi_2 \rangle = c_1 \langle \Psi | \Psi_1 \rangle + c_2 \langle \Psi | \Psi_2 \rangle$ for any vectors $|\Psi\rangle, |\Psi_1\rangle, |\Psi_2\rangle$ and complex numbers c_1, c_2 .

Here, Ψ is just a label name of the vector $|\Psi\rangle$, whose meaning will be got from context; $\langle \Psi |$ is a row vector obtained as the complex conjugate transpose of $|\Psi\rangle$. More generally, any single-qubit state can be chosen as a linear combination $|\psi\rangle = a|0\rangle + b|1\rangle$ with $a, b \in \mathbb{C}$, satisfying $|a|^2 + |b|^2 = 1$, which is called a *superposition* over $|0\rangle$ and $|1\rangle$. The coefficients a and b are the *amplitudes* of $|0\rangle$ and $|1\rangle$ respectively, meaning that after measuring $|\psi\rangle$, we would get the basic state $|0\rangle$ with probability $|a|^2$ and get $|1\rangle$ with the remaining probability $1 - |a|^2 = |b|^2$. To characterize multiple-bit information, the tensor product \otimes is introduced, so that quantum n bits are represented by unit vectors in the product Hilbert space $\mathbb{H}^{\otimes n} = \underbrace{\mathbb{H} \otimes \cdots \otimes \mathbb{H}}_{n \text{ copies}}$.

A few popular gates acting on single qubits are:

- the Hadamard gate $H = |+\rangle\langle 0| + |-\rangle\langle 1| = |0\rangle\langle +| + |1\rangle\langle -|$ where $|\pm\rangle = (|0\rangle \pm |1\rangle)/\sqrt{2}$;
- the four Pauli gates $I = |0\rangle\langle 0| + |1\rangle\langle 1| = |+\rangle\langle +| + |-\rangle\langle -|$, $X = |1\rangle\langle 0| + |0\rangle\langle 1|$, $Y = \imath |1\rangle\langle 0| - \imath |0\rangle\langle 1|$ and $Z = |0\rangle\langle 0| - |1\rangle\langle 1|$, where \imath is imaginary unit;
- the phase gate $e^{\imath\alpha} = e^{\imath\alpha}I$ with $\alpha \in [0, 2\pi)$;
- the $\frac{\pi}{4}$ gate $|0\rangle\langle 0| + \imath |1\rangle\langle 1|$ and the $\frac{\pi}{8}$ gate $|0\rangle\langle 0| + e^{\imath\pi/4} |1\rangle\langle 1|$.

The two-qubit CNOT gate is $CX = |0\rangle\langle 0| \otimes I + |1\rangle\langle 1| \otimes X$. All of them are *basic* gates that are supposed to be well prepared in quantum computers.

An important result stated in [22, Subsection 4.5.3] is:

Theorem 2.1 (Universality) *The set of H , phase, $\frac{\pi}{8}$ and CNOT gates is universal.*

This result indicates that any quantum (single-qubit or multiple-qubit) gate can be approximated within an appointed precision ε by a finite composition of Hadamard, phase, $\frac{\pi}{8}$ and CNOT gates. In short, nonbasic gates can be arbitrarily approximated by the four basic ones.

2.2 Rationale of Grover's algorithm

We briefly describe the Grover's algorithm as follows; the whole process is referred to the circuit in Figure 1. Suppose that the database consists of $N = 2^n$ records with index $|0\rangle$ through $|2^n - 1\rangle$. It suffices to use n qubits to index them.

- Firstly, we apply the Hadamard gate $H^{\otimes n}$ to create the uniform superposition $|\psi_0\rangle = \frac{1}{\sqrt{N}} \sum_{i=0}^{N-1} |i\rangle$ over all N records. This superposition can be reformulated as

$$|\psi_0\rangle = \sqrt{\frac{M}{N}} |\text{goal}\rangle + \sqrt{\frac{N-M}{N}} |\text{nongoal}\rangle = \sin \frac{\theta}{2} |\text{goal}\rangle + \cos \frac{\theta}{2} |\text{nongoal}\rangle, \quad (1)$$

where $|\text{goal}\rangle$ is a state with label name 'goal' denoting the uniform superposition over all M goal records, $|\text{nongoal}\rangle$ is the uniform superposition over the remaining $N - M$ nongoal ones, and $\theta = 2 \arcsin \sqrt{M/N}$. When performing a quantum search, an oracle function O_G is involved to identify goal states and nongoal ones such that we can explicitly define $|\text{goal}\rangle = \frac{1}{\sqrt{M}} \sum_{O_G(i)=\text{goal}} |i\rangle$ and $|\text{nongoal}\rangle = \frac{1}{\sqrt{N-M}} \sum_{O_G(j)=\text{nongoal}} |j\rangle$. The amplitudes of $|\text{goal}\rangle$ and $|\text{nongoal}\rangle$ in $|\psi_0\rangle$ are $\sin \frac{\theta}{2} = \sqrt{M/N}$ and $\cos \frac{\theta}{2} = \sqrt{(N-M)/N}$, respectively. If we measure it, we would get some goal record with probability $\frac{M}{N}$, which usually is too low to be satisfactory. So we amplify it by the following iteration operation.

- The so-called *Grover iterations* G are applied times by times to amplify the amplitude of $|\text{goal}\rangle$ in the resulting superposition $|\psi_j\rangle$. Particularly, the j th Grover iteration brings the amplitude $\sin(\frac{2j-1}{2}\theta)$ to $\sin(\frac{2j+1}{2}\theta)$. After applying $T = \lfloor \frac{\pi}{4} \cdot \sqrt{N/M} \rfloor$ times of Grover iterations, we can get the amplitude of $|\text{goal}\rangle$ at least $\sin(\frac{\pi}{2} \pm \frac{\theta}{2})$, which is a local optimum.

Although the local optimum is close to the perfect amplitude $\sin \frac{\pi}{2} = 1$, it does not guarantee to achieve the success probability $1 - \varepsilon$ for a user-specified error tolerance ε . Whereas, the latter is indeed the error-bounded quantum search problem to be studied in the paper.

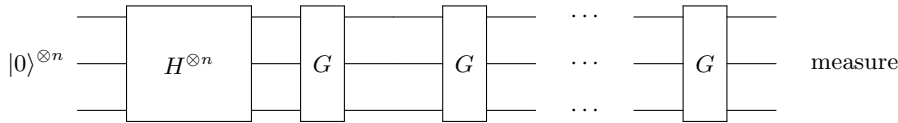


Figure 1: Process of Grover's algorithm

From the geometric viewpoint, the aforementioned gates can be interpreted using the plane spanned by the orthonormal vectors $|\text{goal}\rangle$ and $|\text{nongoal}\rangle$. The orthonormality can be seen from the facts that $\langle i|j\rangle$ is 0 if $i \neq j$, thus $\langle \text{nongoal}|\text{goal}\rangle = 0$. Here, the Grover iteration

$$G = \exp(i\pi |\psi_0\rangle\langle\psi_0|) \cdot \exp(i\pi |\text{nongoal}\rangle\langle\text{nongoal}|) \quad (2)$$

is composed of a rotation through $|\text{nongoal}\rangle$ with angle π followed by a rotation through $|\psi_0\rangle$ with angle π . The former exploits the information $|\text{nongoal}\rangle$ by utilizing the oracle function O_G , so it is a query (a.k.a. oracle) operation. Since the times of applying oracles should be extraordinarily taken into account by the algorithmic aspect, people would like to specify the time complexity of such algorithms in terms of the number of queries, i.e. *query complexity*.

3 An Existing Method

Before stating the method MQI (pronounce ‘more qubits introduced’), we should know the reason why the original Grover’s algorithm fails to achieve the success probability $1 - \varepsilon$. Again, it can be explicitly explained by the geometric viewpoint:

- each Grover iteration makes a rotation of angle θ in the plane spanned by the orthonormal vectors $|\text{goal}\rangle$ and $|\text{nongoal}\rangle$, starting from the initial state $\frac{\theta}{2}$ toward the goal state $\frac{\pi}{2}$ that corresponds to the success probability 1;
- the relatively optimal probability is $\sin^2(\frac{\pi}{2} \pm \frac{\theta}{2}) = 1 - \sin^2(\frac{\theta}{2}) \approx 1 - \frac{\theta^2}{4}$, where the approximation comes from the identity $\sin(\theta) = \theta$ whenever θ is tiny, which might be away from the independently specified threshold $1 - \varepsilon$.

Here, we call the quantity $\sin^2(\frac{\pi}{2} \pm \frac{\theta}{2})$ the *potential* of the current rotation angle θ , meaning that if we are equipped with the rotation of angle θ , the optimal probability can be achieved as least as $\sin^2(\frac{\pi}{2} \pm \frac{\theta}{2})$ after $\lfloor \frac{\pi}{4} \cdot \sin^{-1}(\frac{\theta}{2}) \rfloor = \lfloor \frac{\pi}{4} \cdot \sqrt{N/M} \rfloor$ times of Grover iterations.

In order to achieve the success probability $1 - \varepsilon$, one can narrow the rotation angle θ by inserting plain records to the database, so that the performance is analyzed as:

- every two qubits are introduced to index records,
- the database is quadrupled in size,
- thus the rotation angle per iteration is halved as $2 \arcsin \sqrt{M/4N} \approx \arcsin \sqrt{M/N} = \frac{\theta}{2}$.

Suppose $\varepsilon = \theta^2/4^{k+1}$. Then, by introducing $2k$ qubits to index records, the database is of size $4^k N$, the rotation angle per iteration is narrowed to $\theta/2^k$, and we could achieve the success probability $1 - \varepsilon$, after performing $\lfloor \frac{\pi}{4} \cdot \sqrt{N/M} \cdot 2^k \rfloor = \lfloor \frac{\pi}{2} \cdot \frac{2}{\theta} \cdot 2^k \rfloor = \lfloor \frac{\pi}{2} \cdot \frac{1}{\sqrt{\varepsilon}} \rfloor$ times of Grover iterations. Overall,

- the time complexity of MQI is the tight $\lfloor \frac{\pi}{2} \cdot \frac{1}{\sqrt{\varepsilon}} \rfloor \in \mathcal{O}(1/\sqrt{\varepsilon}) = \mathcal{O}(\sqrt{2}^{\|\varepsilon\|})$ queries where $\|\varepsilon\| = \lceil \log_2(1/\varepsilon) \rceil$ denotes the encoding size of ε ;
- the extra space cost is $2k = \log_2(\theta^2/\varepsilon) - 2 \in \mathcal{O}(\|\varepsilon\| - \log_2 N + \log_2 M)$.

Example 3.1 (Search on a 3-qubit space) Here we apply Grover’s algorithm to find one goal record in an unstructured database of size 8, i.e., the ratio of the goal record out of all ones is $M/N = \frac{1}{8}$, where the records can be indexed by three qubits. During Grover’s search, some facts are listed below:

- the rotation angle of the original Grover iteration is $\theta = 2 \arcsin(1/2\sqrt{2})$,
- after performing $\lfloor \frac{\pi}{2} / (2 \arcsin(1/2\sqrt{2})) \rfloor = 2$ times of Grover iterations, the success probability $P_{\text{succ}} \approx 0.9453$ would be achieved.

Then, if we insert the plain records into the database by increasing the number of qubits, the required number of Grover iterations and the corresponding success probability we achieved are summarized in the Table 1. For instance, when the error tolerance ε is chosen to be 0.01, it suffices to require the potential $\sin^2(\frac{\pi}{2} \pm \frac{\theta}{2}) = (N - M)/N$ greater than 0.99. So we introduce 4 extra qubits, by which the potential is approximately $0.9922 > 0.99$ and the success probability $P_{\text{succ}} \approx 0.9956$ is achieved as we expected. \square

Table 1: Performance of the method MQI

#extra qubits	ratio of goal states	#Grover iterations	potential	success probability
0	1/8	2	0.875	0.9453
1	1/16	3	0.9375	0.9613
2	1/32	4	0.9688	0.9991
4	1/128	8	0.9922	0.9956
6	1/512	17	0.9980	0.9994
8	1/2048	35	0.9995	0.9999

As we all know, the number of available qubits is vital to exploit the capacity of quantum computers. Hence we should save unnecessary space cost as more as possible.

4 Theoretical Guarantee

To avoid the usage of extra working qubits, the method we employ, named ‘more iterations performed’ MIP, is just to perform more times of Grover iterations and thus hit a series of local optima, one of which is hoped to achieve the success probability $1 - \varepsilon$. Here we will explore the realizability of MIP.

It seems to be realizable if the rotation angle θ is an irrational multiple of π , denoted $\theta \notin \mathbb{Q} \cdot \pi$, then the success probability $\sin^2(\frac{2j+1}{2}\theta)$ can approach any appointed value in $[0, 1]$, since the set $\{\frac{2j+1}{2}\theta \bmod \pi : j \in \mathbb{N}\}$ is dense in $[0, \pi)$ by [13, Theorem 439]. But the reality is not the same as what we hope. Considering the case that the ratio M/N is $\frac{1}{4}$, the rotation angle θ is exactly $\frac{\pi}{3}$, which is a rational multiple of π . Are there other such values of M/N ? Fortunately, we can claim:

Lemma 4.1 *All the values of M/N whose rotation angles are rational multiples of π are $\frac{1}{4}$, $\frac{1}{2}$ and $\frac{3}{4}$.*

It entails there are only three exceptions for MIP. One can easily resolve them individually:

- if $M/N = \frac{1}{4}$, then $\theta = \frac{\pi}{3}$, and the success probability 1 would be achieved after once of Grover iteration as $\frac{\theta}{2} + 1 \times \theta = \frac{\pi}{2}$;
- if $M/N = \frac{1}{2}$ or $M/N = \frac{3}{4}$, the goal records are not less than the nongoal ones. The success expectation 1 would be achieved by at most twice of independently classical sampling. Thanks to geometric distribution, we can see that the success probability $1 - \varepsilon$ would be achieved by at most $\|\varepsilon\| = \lceil \log_2(1/\varepsilon) \rceil$ times of independently classical sampling.

Besides them MIP works!

The correctness of Lemma 4.1 is established on algebraic number theory. Recall that:

Definition 4.2 (Algebraic Number) A number α is algebraic if there is an irreducible polynomial $p_\alpha \in \mathbb{Z}[x]$ such that $p_\alpha(\alpha) = 0$.

The degree of α is exactly that of the defining polynomial p_α , which uniquely determined by the irreducibility of p_α . The leading coefficient of a polynomial is the coefficient of the term with the highest degree in that polynomial. For algebraic numbers, we have useful subclasses:

- if the defining polynomial p_α is linear, α is a rational number;
- if p_α is linear and its leading coefficient is 1, α is a rational integer (simply said integer);
- if the leading coefficient of p_α is 1, α is an algebraic integer.

Anyway, algebraic integers are algebraic numbers, and each algebraic number multiplied with an appropriate rational integer would be an algebraic integer.

Example 4.3 Considering a specific angle $\theta = \frac{\pi}{6}$ of the Grover iteration, the initial state is $\sin \frac{\theta}{2} |\text{goal}\rangle + \cos \frac{\theta}{2} |\text{nongol}\rangle$. Then the amplitude of goal records is $\sin \frac{\theta}{2} = \sin \frac{\pi}{12} = \sqrt{2 - \sqrt{3}}/2$. Measuring the initial state, we would get the success probability $\sin^2 \frac{\theta}{2} = (2 - \sqrt{3})/4$. Both are algebraic numbers appearing in the analysis. Particularly, since $\sin \frac{\pi}{12}$ is a root of the irreducible polynomial $p(x) = 16x^4 - 16x^2 + 1$, i. e. $p(\sin \frac{\pi}{12}) = 0$, we can infer that $\sin \frac{\pi}{12}$ is an algebraic number of degree 4. Although $\sin \frac{\pi}{12}$ itself is not an algebraic integer, $2 \sin \frac{\pi}{12}$ obtained as $\sin \frac{\pi}{12}$ multiplied with 2 is an algebraic integer, since it is a root of $p(\frac{x}{2}) = x^4 - 4x^2 + 1$. \square

Theorem 4.4 ([18]) Let $r = k/n$ be a reduced fraction with $n > 2$, and $\phi(n)$ the Euler's function of n (that is the number of positive integers both less than n and coprime to n). Then $2 \cos(2\pi r)$ is an algebraic integer of degree $\phi(n)/2$.

Particularly, we have the following cases:

- $\sin(2\pi r)$ is an algebraic number of degree 1 if and only if $n = 1, 2, 4$;
- $\sin(2\pi r)$ is of degree 2 if and only if $n = 3, 6, 8, 12$;
- $\cos(2\pi r)$ is of degree 1 if and only if $n = 1, 2, 3, 4, 6$;
- $\cos(2\pi r)$ is of degree 2 if and only if $n = 5, 8, 10, 12$.

Now we are ready to give the proof of Lemma 4.1.

Proof In our setting, both $\sin \frac{\theta}{2} = \sqrt{M/N}$ and $\cos \frac{\theta}{2} = \sqrt{(N-M)/N}$ are algebraic numbers of degree at most 2, since their defining polynomials are irreducible factors of $Nx^2 - M$ and $Nx^2 - (N - M)$, respectively. It entails that $\frac{\theta}{2}$ equals $2\pi k/n$ only possibly for

$$n = 1, 2, 3, 4, 6, 8, 12.$$

As $r = k/n$ is a reduced fraction, we know that all candidate values of r are

$$\frac{1}{2}, \frac{1}{3}, \frac{2}{3}, \frac{1}{4}, \frac{3}{4}, \frac{1}{6}, \frac{5}{6}, \frac{1}{8}, \frac{3}{8}, \frac{5}{8}, \frac{7}{8}, \frac{1}{12}, \frac{5}{12}, \frac{7}{12}, \frac{11}{12},$$

among which only

$$r = \frac{1}{6}, \frac{1}{8}, \frac{1}{12}. \quad (3)$$

are qualified, since others do not meet the constraint $0 < 2\pi r = \frac{\theta}{2} = \arcsin \sqrt{M/N} < \frac{\pi}{2}$. The three values of r correspond to the rotation angles

$$\theta = \frac{2\pi}{3}, \frac{\pi}{2}, \frac{\pi}{3}, \quad (4)$$

and thereby the ratios are

$$\frac{M}{N} = \frac{3}{4}, \frac{1}{2}, \frac{1}{4}. \quad (5)$$

5 Algorithmic Analysis

Now we turn to analyze the theoretical performance of MIP. The main result is summarized as Theorem 5.1, whose proof will be delivered later on.

Theorem 5.1 (Performance) *If θ is an irrational multiple of π , the success probability $1 - \varepsilon$ can be achieved within $\mathcal{O}(\sqrt{3}^{\|\varepsilon\|})$ times of Grover iterations.*

The Grover iteration G itself forms a universal gate set, which can be used to approximate the gate mapping the initial state $|\psi_0\rangle = \sin \frac{\theta}{2} |\text{goal}\rangle + \sin \frac{\theta}{2} |\text{nongoal}\rangle$ to the ideal one $|\text{goal}\rangle$, whenever $\theta \notin \mathbb{Q} \cdot \pi$. By [22, Subsection 4.5.3], one can easily see that the performance has the upper bound $\mathcal{O}(1/\varepsilon) = \mathcal{O}(2^{\|\varepsilon\|})$, while we aim to give a tighter bound in Theorem 5.1. We notice that the performance here is in the same exponential hierarchy as MQI in Section 3, which seems that the error-bounded quantum search problem would be **EXP**-hard.

The function $\sin^2(t)$ used to interpret the success probability is of period π , and achieves the maximum 1 at $t = \frac{\pi}{2} + i\pi$ for $i \in \mathbb{Z}$. In the following, we would identify states after j th iterations with $j \in \mathbb{N}$ by angles in $[0, \pi)$ for brevity. As an effective identification, it requires that every state after j th iteration is identified by a unique angle in $[0, \pi)$. Here, the set of all states after j th iterations is countable while the set of all angles in $[0, \pi)$ is uncountable, and the states after different times of iterations are different due to $\theta \notin \mathbb{Q} \cdot \pi$, so the identification is valid. The proof of Theorem 5.1 is based on the inductive construction:

1. *basic step* — From the initial state $\frac{\theta}{2}$, we count the required numbers of iterations to hit two states $\frac{\pi}{2} - l_0$ and $\frac{\pi}{2} + u_0$ with $0 < l_0, u_0 < \theta$, which are the edges of a sector containing $\frac{\pi}{2}$.
2. *inductive step* — From the state $\frac{\pi}{2} - l_i$, we count the required numbers of iterations to hit two states $\frac{\pi}{2} - l_{i+1}$ and $\frac{\pi}{2} + u_{i+1}$ with $0 < l_{i+1}, u_{i+1} < \theta/2^{i+1}$, which are the edges of a sector containing $\frac{\pi}{2}$.

The sequential refinement in sectors would terminate whenever the resulting sector is sufficiently narrow. The details are provided as follows.

Basic step of refinement From the initial state $\frac{\theta}{2}$, we need $T_0 = \lfloor (\frac{\pi}{2} - \frac{\theta}{2})/\theta \rfloor$ times of iterations to hit some state $\frac{\pi}{2} - l_0$ satisfying $0 < l_0 < \theta$; and need additionally $S_0 = 1$ of iterations to hit the state $\frac{\pi}{2} + u_0$ with $u_0 = \theta - l_0$. The required number of iterations is

$$\underbrace{T_0}_{\text{hit one edge of } \mathfrak{S}_0} + \underbrace{S_0}_{\text{hit another edge}} \quad (6)$$

to yield that:

- $\langle \frac{\pi}{2} - l_0, \frac{\pi}{2} + u_0 \rangle$ forms a sector \mathfrak{S}_0 of angle $\theta_0 = \theta$, and
- exactly one of l_0 and u_0 is less than $\frac{\theta}{2}$.

The process is shown in Figure 2, in which the X -coordinate axis measures $\cos(\frac{2j+1}{2}\theta)$ and the Y -coordinate one measures $|\sin(\frac{2j+1}{2}\theta)|$, where we relabel the coordinate quantities to intuitively reflect the success probability under the number of iterations without loss of information. So the states after any times of Grover iterations would appear in the above half circle; the success probability achieves 1 if and only if the state coincides with the Y -coordinate axis.

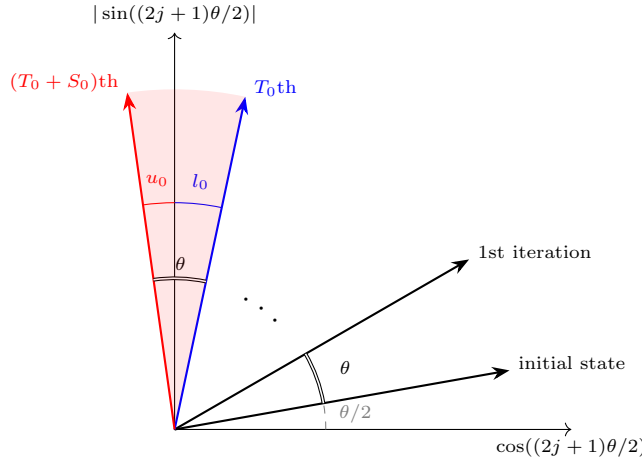


Figure 2: Basic step of refinement

First round of refinement As $\theta \notin \mathbb{Q} \cdot \pi$, we have that $S_1 = \lceil \frac{\pi}{\theta} \rceil$ is the least value of $j \in \mathbb{Z}^+$, satisfying $0 < j \cdot \theta \bmod \pi < \theta_0$, where ' $j \cdot \theta \bmod \pi$ ' denotes the remainder of $j \cdot \theta$ modulo π . It entails that from the state $\frac{\pi}{2} - l_0$, we need S_1 times of iterations to hit an inner state $\frac{\pi}{2} + m_0$ in the previous sector \mathfrak{S}_0 . Further, we discuss it in two cases:

1. the inner state $\frac{\pi}{2} + m_0$ is closer to the edge state $\frac{\pi}{2} - l_0$ than $\frac{\pi}{2} + u_0$,
2. the inner state $\frac{\pi}{2} + m_0$ is closer to the edge state $\frac{\pi}{2} + u_0$ than $\frac{\pi}{2} - l_0$.

For the former, we consider the angle $\theta_1 = m_0 + l_0$ of the sector spanned by the two edges $\frac{\pi}{2} + m_0$ and $\frac{\pi}{2} - l_0$, that is the narrower subsector of \mathfrak{S}_0 split by the inner state $\frac{\pi}{2} + m_0$. The

$$\begin{aligned} \underbrace{T_0 + T_1}_{\text{hit one edge of } \mathfrak{S}_1} + \underbrace{S_1}_{\text{hit another edge}} &= \left\lfloor \frac{\frac{\pi}{2} - \frac{\theta}{2}}{\theta} \right\rfloor + \left\lfloor \frac{\theta_0}{\theta_1} \right\rfloor \cdot \left\lceil \frac{\pi}{\theta_0} \right\rceil + \left\lceil \frac{\pi}{\theta_0} \right\rceil \\ &= \left\lfloor \frac{\pi - \theta}{2\theta} \right\rfloor + \left\lfloor \frac{\theta_0}{\theta_1} \right\rfloor \cdot \left\lceil \frac{\pi}{\theta_0} \right\rceil \end{aligned} \quad (7)$$

- $\langle \frac{\pi}{2} - l_1, \frac{\pi}{2} + u_1 \rangle$ forms a sector \mathfrak{S}_1 of angle $\theta_1 < \frac{\theta_0}{2}$, and
- exactly one of l_1 and u_1 is less than $\frac{\theta_1}{2}$.

The figure consists of two polar coordinate diagrams. The left diagram shows a vector starting at the origin and ending at a point labeled $(T_0 + S_1)th$. A dashed blue arc represents the T_0th iteration, and a solid blue arc represents the $(T_0 + S_1)th$ iteration. The angle between the radial lines is θ_1 , and the radial distances are l_0 and l_1 . The right diagram shows a vector starting at the origin and ending at a point labeled $(T_0 + 2S_1)th$. A dashed blue arc represents the T_0th iteration, and a solid blue arc represents the $(T_0 + 2S_1)th$ iteration. The angle between the radial lines is θ_1 , and the radial distances are l_0 and l_1 . Both diagrams have a horizontal axis labeled $\cos((2j+1)\theta/2)$ and a vertical axis labeled $|\sin((2j+1)\theta/2)|$.

For the latter, we consider the angle $\theta_1 = u_0 - m_0$ of the sector spanned by $\frac{\pi}{2} + m_0$ and $\frac{\pi}{2} + u_0$. By the known fact that $S_1 - S_0$ times of iterations takes state from $\frac{\pi}{2} + u_0$ to $\frac{\pi}{2} + u_0 - \theta_1 = \frac{\pi}{2} + m_0$, we can deduce that $i \times (S_1 - S_0)$ times of iterations takes state from $\frac{\pi}{2} + u_0$ to $\frac{\pi}{2} + u_0 - i \times \theta_1$, since every $S_1 - S_0$ times of iterations makes a reverse rotation of net angle θ_1 . From the state $\frac{\pi}{2} - l_0$, we need at most $T'_1 = S_0 + \lfloor \theta_0 / \theta_1 \rfloor \cdot (S_1 - S_0)$ times of iterations to hit some state

$\frac{\pi}{2} + u_1$ satisfying $0 < u_1 < \theta_1$, where u_1 is chosen to be $u_0 - \lfloor u_0/\theta_1 \rfloor \cdot \theta_1$; and need additionally $S_1 - S_0$ of iterations to hit the state $\frac{\pi}{2} - l_1$ with $l_1 = \theta_1 - u_1$. Up to the current refinement, the required number of iterations is bounded from above by

$$\begin{aligned}
 \underbrace{T_0 + T'_1}_{\text{hit one edge of } \mathfrak{S}_1} + \underbrace{S_1 - S_0}_{\text{hit another edge}} &= \left\lfloor \frac{\frac{\pi}{2} - \frac{\theta_0}{2}}{\theta_0} \right\rfloor + 1 + \left\lfloor \frac{\theta_0}{\theta_1} \right\rfloor \cdot \left\lfloor \frac{\pi}{\theta_0} \right\rfloor + \left\lceil \frac{\pi}{\theta_0} \right\rceil - 1 \\
 &= \left\lfloor \frac{\pi - \theta_0}{2\theta_0} \right\rfloor + \left\lceil \frac{\theta_0}{\theta_1} \right\rceil \cdot \left\lfloor \frac{\pi}{\theta_0} \right\rfloor + 1 \\
 &< T_0 + T_1 + S_1.
 \end{aligned} \tag{8}$$

The process is shown in Figure 4, in which we would make a reverse rotation of net angle θ_1 after $S_1 - S_0$ times of iterations.

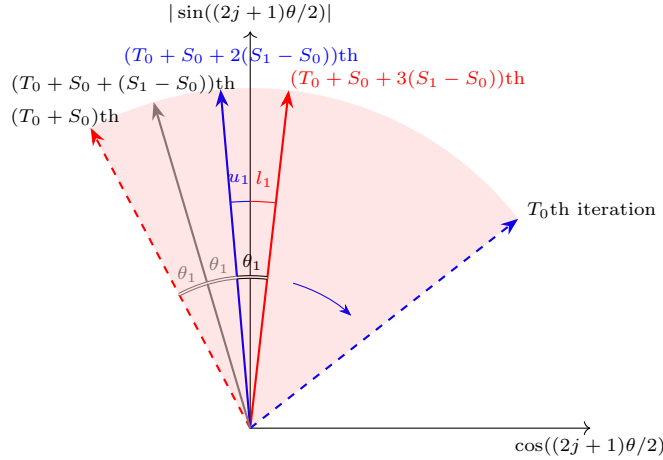


Figure 4: First round of refinement when $\frac{\pi}{2} + m_0$ is close to $\frac{\pi}{2} + u_0$

Example 5.2 Recall the quantum search process on the 3-qubit space in Example 3.1, where we have embraced the fact that the rotation angle of each Grover iteration is $\theta = 2 \arcsin(1/2\sqrt{2})$. We show the intermediate results of the refinement process as follows.

- For the basic step of refinement, from the initial state $\frac{\theta}{2} = \arcsin(1/2\sqrt{2})$, we hit
 - the state $\frac{\pi}{2} - l_0 = \frac{3}{2}\theta = 3 \arcsin(1/2\sqrt{2}) \approx 62.114^\circ$ after once of Grover iteration, and
 - another state $\frac{\pi}{2} + u_0 = \frac{5}{2}\theta = 5 \arcsin(1/2\sqrt{2}) \approx 103.524^\circ$ after additional once.

Then it is obvious to see that the state $\frac{\pi}{2}$ is covered by the sector $\mathfrak{S}_0 = \langle \frac{\pi}{2} - l_0, \frac{\pi}{2} + u_0 \rangle$.

- For the first round of refinement, from the state $\frac{\pi}{2} - l_0$, there is a state $\frac{\pi}{2} + m_0 = 13 \arcsin(1/2\sqrt{2}) - \pi \approx 89.163^\circ \in \mathfrak{S}_0$ after $S_1 = \lceil \frac{\pi}{\theta} \rceil = 5$ times of Grover iterations. Here the inner state $\frac{\pi}{2} + m_0$ is closer to the edge state $\frac{\pi}{2} + u_0$ than $\frac{\pi}{2} - l_0$; and m_0 is negative. Thus, from the state $\frac{\pi}{2} - l_0$, we hit

- the state $\frac{\pi}{2} - l_1 = \frac{\pi}{2} + m_0$ after 5 times of Grover iterations, and
- another state $\frac{\pi}{2} + u_1 = \frac{\pi}{2} + u_0$ intermediately.

The sector \mathfrak{S}_0 is halved to $\mathfrak{S}_1 = \langle \frac{\pi}{2} - l_1, \frac{\pi}{2} + u_1 \rangle$, which still covers the state $\frac{\pi}{2}$. \square

Inductive rounds of refinement The inductive step of refinement can be formulated as:

Lemma 5.3 *Let $\mathfrak{S}_i = \langle \frac{\pi}{2} - l_i, \frac{\pi}{2} + u_i \rangle$ be a sector of angle θ_i as constructed above, for $i \geq 1$. Then, from the state $\frac{\pi}{2} - l_i$, we need at most*

1. $S_{i+1} = \lceil \theta_{i-1}/\theta_i \rceil \cdot S_i$ times of iterations to hit an inner state $\frac{\pi}{2} + m_i$ in \mathfrak{S}_i ;
2. $T_{i+1} = \lfloor \theta_i/\theta_{i+1} \rfloor \cdot S_{i+1}$ times of iterations to hit one edge of \mathfrak{S}_{i+1} , where $\theta_{i+1} = \min\{m_i + l_i, u_i - m_i\}$, and additionally S_{i+1} times of iterations to hit another, so that the resulting \mathfrak{S}_{i+1} is a sector of angle $\theta_{i+1} < \frac{\theta_i}{2}$.

Overall, the required number of iterations is bounded from above by

$$\underbrace{T_0 + T_1 + \cdots + T_{i+1}}_{\text{hit one edge of } \mathfrak{S}_{i+1}} + \underbrace{S_{i+1}}_{\text{hit another edge}}. \quad (9)$$

Proof To prove the first item, we list the known factors that every S_{i-1} (possibly less) times of iterations makes a rotation of net angle θ_{i-1} ; and that every S_i times of iterations makes a rotation of net angle ϑ ; further,

- if $\vartheta < \frac{\theta_{i-1}}{2}$, then θ_i is exactly ϑ ;
- otherwise θ_i is $\theta_{i-1} - \vartheta$, which is obtained by performing $S_i - S_{i-1}$ times of iterations.

We dealt with the two cases respectively as follows.

- For the former case, $\lceil \theta_{i-1}/\theta_i \rceil$ times of θ_i amounts to some net angle in the range $(\theta_{i-1}, \theta_{i-1} + \theta_i)$. So, at most $\lceil \theta_{i-1}/\theta_i \rceil \cdot S_i - S_{i-1}$ times of iterations would make a rotation of net angle less than θ_i .
- For the latter case, $\lceil \theta_{i-1}/\theta_i \rceil$ times of $\theta_i - \theta_{i-1}$ amounts to some net angle in the range $(-\theta_{i-1} - \theta_i, -\theta_{i-1})$. So, at most $\lceil \theta_{i-1}/\theta_i \rceil \cdot (S_i - S_{i-1}) + S_{i-1}$ times of iterations would make a reverse rotation of net angle less than θ_i .

Anyway, from the state $\frac{\pi}{2} - l_i$, at most S_{i+1} times of iterations could hit some inner state $\frac{\pi}{2} + m_i$ in \mathfrak{S}_i , since $\lceil \theta_{i-1}/\theta_i \rceil \cdot S_i - S_{i-1} < \lceil \theta_{i-1}/\theta_i \rceil \cdot S_i = S_{i+1}$ and

$$\underbrace{S_{i-1}}_{\text{move from } \frac{\pi}{2} - l_i \text{ to } \frac{\pi}{2} + u_i} + \underbrace{\left\lceil \frac{\theta_{i-1}}{\theta_i} \right\rceil \cdot (S_i - S_{i-1}) + S_{i-1}}_{\text{move from } \frac{\pi}{2} + u_i \text{ to } \frac{\pi}{2} + m_i} < \left\lceil \frac{\theta_{i-1}}{\theta_i} \right\rceil \cdot S_i = S_{i+1} \quad (10)$$

holds for $\lceil \theta_{i-1}/\theta_i \rceil > 2$.

To prove the second item, we know that every S_{i+1} (possibly less) times of iterations makes a rotation of net angle θ_{i+1} . So $\frac{\pi}{2}$ must fall into one of $\lceil \theta_i/\theta_{i+1} \rceil$ successive sectors of equal angle θ_{i+1} , starting from $\frac{\pi}{2} - l_i$, whose two edges would be hit after T_{i+1} times and $T_{i+1} + S_{i+1}$ times of iterations respectively. \square

The whole process with over-estimated number of iterations is intuitively summarized in Figure 5.

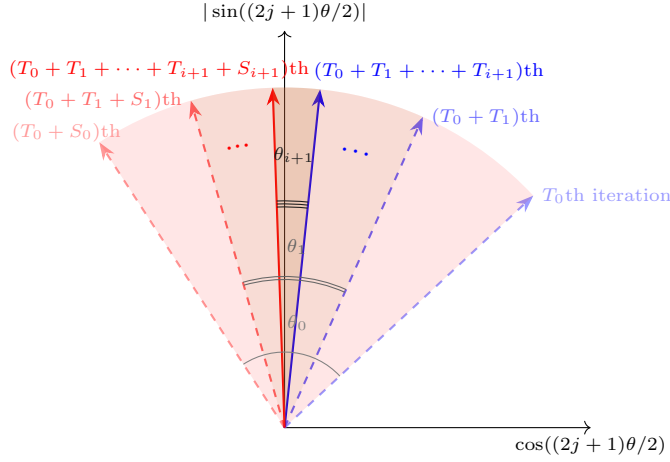


Figure 5: Inductive rounds of refinement

By the recursive definition of $S_{i+1} = \lceil \theta_{i-1}/\theta_i \rceil \cdot S_i$ with the initial condition $S_1 = \lceil \pi/\theta_0 \rceil$, it is not hard to see

$$\begin{aligned} S_{i+1} &= \left\lceil \frac{\theta_{i-1}}{\theta_i} \right\rceil \cdot S_i = \left\lceil \frac{\theta_{i-1}}{\theta_i} \right\rceil \cdots \left\lceil \frac{\theta_0}{\theta_1} \right\rceil \cdot \left\lceil \frac{\pi}{\theta_0} \right\rceil \\ &< \frac{3\theta_{i-1}}{2\theta_i} \cdots \frac{3\theta_0}{2\theta_1} \cdot \left\lceil \frac{\pi}{\theta_0} \right\rceil = \frac{\theta_0}{\theta_i} \cdot \left\lceil \frac{\pi}{\theta_0} \right\rceil \cdot \left(\frac{3}{2}\right)^i, \end{aligned} \quad (11)$$

since $\theta_0/\theta_1, \dots, \theta_{i-1}/\theta_i$ are fractions greater than 2 and thus the ceiling operation would increase them by less than halves of their respective values. The inequality will be used right now.

Last round of refinement Suppose $\varepsilon = \theta_m^2/4$, implying that m rounds of refinement ensure the error toleration ε . Let k be the least integer such that $\theta/2^k \leq \theta_m$. We have $m < k \leq \log_2(\theta/2\sqrt{\varepsilon})$. By Lemma 5.3, the required number of iterations is bounded from above by

$$\begin{aligned} &\underbrace{T_0 + T_1 + \cdots + T_m}_{\text{hit one edge of } \mathfrak{S}_m} + \underbrace{S_m}_{\text{hit another edge}} \\ &= \left\lceil \frac{\pi - \theta}{2\theta} \right\rceil + \left\lceil \frac{\theta_0}{\theta_1} \right\rceil \cdot S_1 + \left\lceil \frac{\theta_1}{\theta_2} \right\rceil \cdot S_2 + \cdots + \left\lceil \frac{\theta_{m-1}}{\theta_m} \right\rceil \cdot S_m + S_m \end{aligned}$$

$$\begin{aligned}
&< S_1 + \left\lfloor \frac{\theta_0}{\theta_1} \right\rfloor \cdot S_1 + \left\lfloor \frac{\theta_1}{\theta_2} \right\rfloor \cdot S_2 + \cdots + \left\lfloor \frac{\theta_{m-1}}{\theta_m} \right\rfloor \cdot S_m + S_m \\
&= S_2 + \left\lfloor \frac{\theta_1}{\theta_2} \right\rfloor \cdot S_2 + \cdots + \left\lfloor \frac{\theta_{m-1}}{\theta_m} \right\rfloor \cdot S_m + S_m \\
&= S_3 + \cdots + \left\lfloor \frac{\theta_{m-1}}{\theta_m} \right\rfloor \cdot S_m + S_m \\
&= \cdots \\
&= S_m + \left\lfloor \frac{\theta_{m-1}}{\theta_m} \right\rfloor \cdot S_m + S_m = \left\lceil \frac{\theta_{m-1}}{\theta_m} \right\rceil \cdot S_m + S_m \\
&= \left\lceil \frac{\pi}{\theta_0} \right\rceil \cdot \left\lceil \frac{\theta_0}{\theta_1} \right\rceil \cdot \left\lceil \frac{\theta_1}{\theta_2} \right\rceil \cdots \left\lceil \frac{\theta_{m-1}}{\theta_m} \right\rceil + \left\lceil \frac{\pi}{\theta_0} \right\rceil \cdot \left\lceil \frac{\theta_0}{\theta_1} \right\rceil \cdot \left\lceil \frac{\theta_1}{\theta_2} \right\rceil \cdots \left\lceil \frac{\theta_{m-2}}{\theta_{m-1}} \right\rceil \\
&< \left\lceil \frac{\pi}{\theta_0} \right\rceil \cdot \left\lceil \frac{\theta_0}{\theta_1} \right\rceil \cdot \left\lceil \frac{\theta_1}{\theta_2} \right\rceil \cdots \left\lceil \frac{\theta_{m-1}}{\theta_m} \right\rceil \cdot (1 + \frac{1}{2}) \\
&< \left\lceil \frac{\pi}{\theta} \right\rceil \cdot \frac{\theta}{\theta_m} \cdot (\frac{3}{2})^{m+1} = \left\lceil \frac{\pi}{\theta} \right\rceil \cdot \frac{\theta}{2\sqrt{\varepsilon}} \cdot (\frac{3}{2})^{m+1} \\
&\leq \left\lceil \frac{\pi}{\theta} \right\rceil \cdot \frac{\theta}{2\sqrt{\varepsilon}} \cdot (\frac{3}{2})^{\log_2(\theta/2\sqrt{\varepsilon})} = \left\lceil \frac{\pi}{\theta} \right\rceil \cdot \left(\frac{\theta}{2\sqrt{\varepsilon}} \right)^{\log_2 3}, \tag{12}
\end{aligned}$$

in which

- the first inequality simply follows by $\lfloor (\pi - \theta)/2\theta \rfloor < \lceil \pi/\theta_0 \rceil = S_1$,
- the second inequality follows by $\theta_{m-1}/\theta_m > 2$,
- the third inequality comes from Inequality (11), and
- the last inequality follows by $m + 1 \leq \log_2(\theta/2\sqrt{\varepsilon})$.

That is, it requires at most $\lceil \pi/\theta \rceil \cdot (\theta/2\sqrt{\varepsilon})^{\log_2 3} \in \mathcal{O}((1/\sqrt{\varepsilon})^{\log_2 3}) = \mathcal{O}(\sqrt{3}^{\lceil \varepsilon \rceil})$ times of Grover iterations to achieve the success probability $1 - \varepsilon$ without any extra space. Hence, the proof of Theorem 5.1 is completed. \square

Example 5.4 We continue to analyze the performance of MIP on the 3-qubit space in Example 3.1. The results are summarized in Table 2.

Table 2: Performance of MIP

i th round	θ_i	$T_i + S_i$	potential	sector \mathfrak{S}_i	#iter. to hit \mathfrak{S}_i	succ. prob.
0	41.410°	1+1	0.875	$\langle 62.114^\circ, 103.524^\circ \rangle$	1+1	0.945313
1	14.362°	10+5	0.984375	$\langle 89.163^\circ, 103.524^\circ \rangle$	1+4	0.999786
2	1.675°	120+15	0.999786	$\langle 88.450^\circ, 90.125^\circ \rangle$	104+13	0.999995
3	0.713°	270+135	0.999961	$\langle \mathbf{89.412^\circ}, \mathbf{90.125^\circ} \rangle$	0+113	0.999995
4	0.250°	810+405	0.999995	$\langle 89.911^\circ, 90.161^\circ \rangle$	426+213	0.999997

For instance, suppose that we are given the error tolerance $\varepsilon = 0.0001$. It suffices to require the potential bounded from below by 0.9999, entailing that the ultimate sector should be of angle less than $2 \arcsin(1/\sqrt{0.0001}) \approx 1.146^\circ$. As shown in Table 2, after 3 rounds of refinement, the potential is approximately $0.999961 > 0.9999$. In practice, from initial state $\frac{\theta}{2}$ to hit the two edge states of \mathfrak{S}_3 , the required number of Grover iterations is the sum $1+1+104+0+113 = 219$ over the blue numbers in the sixth column, which has the theoretical bound (12) that is the sum $1 + 10 + 120 + 270 + 135 = 536$ over the red numbers in the third column.

Besides, we can see from Table 2 that two successive rounds of refinement would narrow the sector dramatically, not merely to be one fourth. For example, \mathfrak{S}_2 is only $1.675^\circ/41.410^\circ \approx 0.04$ of \mathfrak{S}_0 in the size, and \mathfrak{S}_3 is only $0.713^\circ/14.362^\circ \approx 0.05$ of \mathfrak{S}_1 in the size. That might be used to get a tight complexity of the method MIP employed in the paper.

6 Experimental Results

In this section we experiment the existing method MQI and the employed one MIP, and compare their performance on a series of data sets with various scales. With the rapid advancement of technology, massive amounts of data are continuously generated to meet the requirements in fields. Among them, many of the data sets are defined by unstructured and large volumes, such as various and unpredictable posts in social media platforms. The employed method MIP will be validated as a promising approach to handle large volumes of those data in the context of quantum.

We extract information from two real-world data sets Aviation Safety Reporting System (ASRS) [3] and the public Amazon review (PAR) [10, 21], and conduct experiments on them. The ASRS database is the world’s largest repository of aviation safety information managed by frontline personnel. The total amount of records exported from the ASRS database is nearly 1,000,000. The PAR database is a widely-used benchmark in e-commerce analysis. The database from [10] has a total amount of up to 199,298,798 review records, involved with 13,727,767 users and 6,926,608 items.

In order to demonstrate the scalability regularly, we rescale the total number of records in the ASRS database (resp. PAR database) to 2^{20} (resp. 2^{30}) by proportionally duplicating records. Thus, the number of goal records in two databases increases accordingly. All the experimental queries from ASRS and PAR databases are collected in Tables 3 and 4.

Table 3: Queries in ASRS database

query description	#goal records	
	original	rescaled
flight condition = “marginal” lighting = “dusk” weather = “snow” or “rain”	27	29
flight condition = “marginal” lighting = “night”	744	781
flight condition = “mixed”	10044	10532

Table 4: Queries in PAR database

product title	#goal records	
	original	rescaled
Amazon eGift Card — Give Thanks	7	38
Talbots Gift Card	41	221
Rugby Acne Medication 10% 42.5gm	83	448
Avalon Grapefruit and Geranium Smoothing Shampoo, 11oz	761	4100
Pre de Provence Artisanal French Soap Bar Enriched with Shea Butter	2959	17936

We simulate the experiments that search for various amount of goal records in databases of three scales:

- small-scale ($N \leq 2^{20}$) consisting of illustrative sample instances and ASRS database,
- medium-scale ($N = 2^{30}$) consisting of public Amazon review,
- large-scale ($N = 2^{40}$) consisting of gigantic random instances.

The detailed results are summarized in Table 5 and those of more instances with random goal ratios in Figure 6. Overall, the experimental results well reveal that both quantum search methods MQI and MIP are promising and competitive against the classical one in terms of query complexity. In particular, the larger the volumes of the database and the smaller the goal ratio, the more superiority the queries in a quantum system show over the ones in a classical system, since the query complexity of classical unstructured searching completely depends on the size of both database and goal records. The experiments on the databases of various sizes also show the validity, efficiency and scalability of the two methods, which are reflected by the final achieved success probability with an appointed error tolerance and the required numbers of Grover iterations, i.e. the query complexity. The resource code and complete data are available at https://github.com/melonysuga/Codes_for_EAA.

Validity and scalability of the two methods From Table 5, we can see that the success probability of MIP under the appointed error tolerance are achieved in all instances with different goal ratios at three scales. For MQI, seen from the fourth column of Table 5, the number of qubits added may even exceed the number required for indexing original records as the demand for accuracy increases. For example, from the sixth line of the table, we can see that the number of extra qubits 10 is greater than the original number of qubits $\lceil \log_2 112 \rceil = 7$. At the same time, each new request for error tolerance leads re-implementation of the oracle applied to the database where plain records are added. As can be seen from both Table 5 and Figure 6, in some experimental instances with the same goal ratio and error tolerance, MIP requires the same number of iterations as MQI, sometimes even less. For example, in the last row of the “public Amazon review” block in Table 5, the number of iterations in MIP is less than one-eighth of that of MQI. In the great majority of cases, MIP requires more times of iterations than MQI. However, in the experiments corresponding to each subfigure of Figure 6, 168 random instances at scale $N = 2^{10}$ and 1,229 random instances at each scale $N = 2^{20}, 2^{30}, 2^{40}$ illustrate the fact that the required number of iterations when applying MIP in most cases is greatly less than the theoretical bound, which implies the time complexity $\mathcal{O}(\sqrt{3}^{\|\epsilon\|})$ of MIP is not tight for the average case. The information of theoretical iteration number is omitted in the figures for conciseness. We also tested on more instances and got the similar experimental results, and all detailed information can be found in the link given before. We have reason to believe that MIP is applicable for more larger-scale databases with different goal ratios.

Table 5: Performance comparison between MQI and MIP

scenario	ratios	tolerance	MQI			MIP		
			#qubits	#iter.	succ. prob.	theoret. bound	#iter.	succ. prob.
illustrative sample instances	1/8	10^{-2}	2	4	$1 - 0.8 \cdot 10^{-3}$	16	6	$1 - 0.2 \cdot 10^{-3}$
	1/8	10^{-4}	5	13	$1 - 0.53 \cdot 10^{-4}$	146	119	$1 - 0.47 \cdot 10^{-5}$
	3/112	10^{-4}	3	14	$1 - 0.58 \cdot 10^{-4}$	2094	568	$1 - 0.21 \cdot 10^{-5}$
	3/112	10^{-6}	10	154	$1 - 0.41 \cdot 10^{-6}$	85794	22639	$1 - 0.1 \cdot 10^{-8}$
ASRS	29/2 ²⁰	10^{-7}	4	597	$1 - 0.1 \cdot 10^{-6}$	7025	2837	$1 - 0.6 \cdot 10^{-7}$
	781/2 ²⁰	10^{-7}	8	460	$1 - 0.27 \cdot 10^{-7}$	13020	2618	$1 - 0.68 \cdot 10^{-7}$
	10532/2 ²⁰	10^{-7}	12	502	$1 - 0.24 \cdot 10^{-7}$	16791	6673	$1 - 0.67 \cdot 10^{-9}$
	38/2 ³⁰	10^{-9}	3	11808	$1 - 0.39 \cdot 10^{-10}$	62624	29224	$1 - 0.69 \cdot 10^{-9}$
public Amazon review	221/2 ³⁰	10^{-9}	3	4897	$1 - 0.11 \cdot 10^{-9}$	50212	32892	$1 - 0.69 \cdot 10^{-9}$
	448/2 ³⁰	10^{-9}	7	13756	$1 - 0.61 \cdot 10^{-10}$	57151	32829	$1 - 0.72 \cdot 10^{-9}$
	4100/2 ³⁰	10^{-9}	9	9095	$1 - 0.21 \cdot 10^{-9}$	55877	52652	$1 - 0.47 \cdot 10^{-9}$
	17936/2 ³⁰	10^{-9}	11	8696	$1 - 0.82 \cdot 10^{-10}$	1731	960	$1 - 0.59 \cdot 10^{-9}$
gigantic random instances	743/2 ⁴⁰	10^{-12}	4	120852	$1 - 0.88 \cdot 10^{-12}$	15680805	5226867	$1 - 0.5 \cdot 10^{-14}$
	6007/2 ⁴⁰	10^{-12}	5	60109	$1 - 0.8 \cdot 10^{-13}$	1774541	860688	$1 - 0.8 \cdot 10^{-12}$
	7937/2 ⁴⁰	10^{-12}	8	147905	$1 - 0.52 \cdot 10^{-12}$	3596109	1691658	$1 - 0.1 \cdot 10^{-13}$
	97169/2 ⁴⁰	10^{-12}	14	338171	$1 - 0.41 \cdot 10^{-12}$	948477	472910	$1 - 0.9 \cdot 10^{-12}$
	799993/2 ⁴⁰	10^{-12}	15	166675	$1 - 0.12 \cdot 10^{-12}$	2784182	639928	$1 - 0.95 \cdot 10^{-12}$

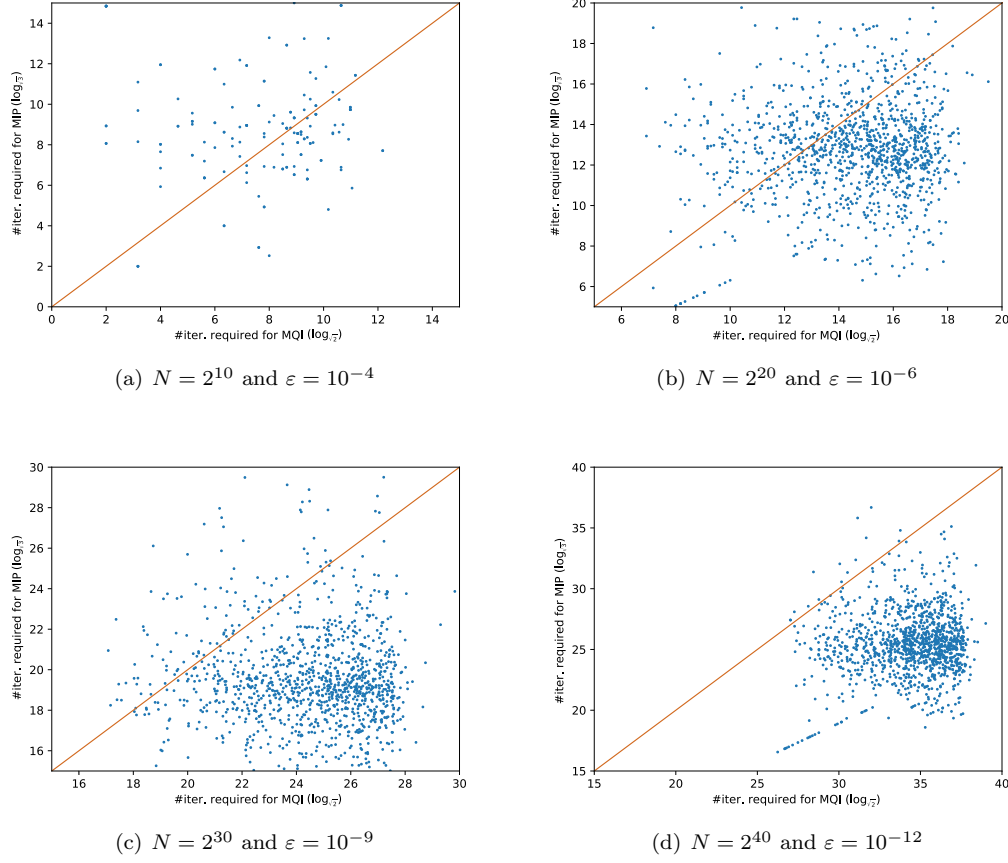


Figure 6: Performance comparison on different parameters

Rate of the sector angles' decreasing during refinement In Figure 7, we reveal that the effect on the angles of refining sectors by calculating the averaged ratios between the angles of two sectors in three random instances, as used in Table 5, at three scales. The solid lines demonstrate the trend of successive ratios θ_i/θ_{i-1} and the dashed ones the trend of accumulative ratios $\theta_{i+1}/\theta_{i-1}$, for $i = 1$ through 10. The X-coordinate axis represents the number of refinement. Apparently, the value of each successive ratio is much less than one-half, and the average of all successive ratios in experiments shows less than one-third, which is demonstrated by a purple dash-dot line in the figure. Besides, after accumulating two rounds of refinement, the ratio value of two sector angles fluctuates around one-tenth, which is exactly what we expected earlier. The average of all accumulative ratios, demonstrated by a purple dotted line in the figure, is less than one-tenth in our experiments. Hence the practical performance of MIP is likely to be $\mathcal{O}(\sqrt{2}^{\|\varepsilon\|})$ in the average case.

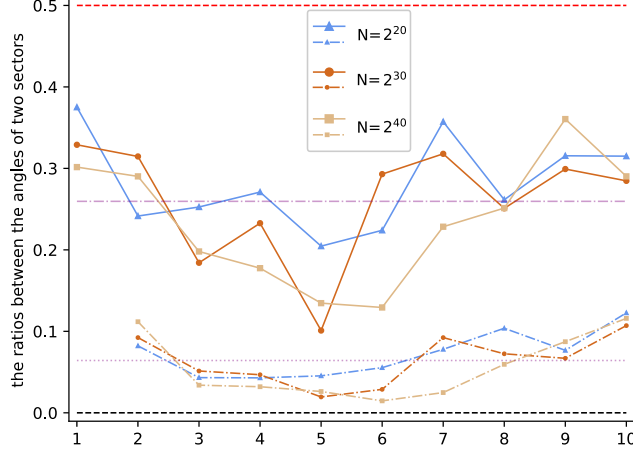


Figure 7: Effect on the angles of refining sectors

7 Concluding Remarks

The existing method MQI described in Section 3 has the time complexity $\mathcal{O}(\sqrt{2}^{\|\varepsilon\|})$, which is tight since the maximal success probability is achieved after almost $\sqrt{2}^{\|\varepsilon\|}$ times of Grover iterations. However, the time complexity $\mathcal{O}(\sqrt{3}^{\|\varepsilon\|})$ of the employed method MIP in Theorem 5.1 is just an upper bound, which does not mean it is tight. A lot of random examples from ASRS and public Amazon review databases in Section 6 have validated this point. It seems to be a long journey to tighten the time complexity. We left it as one of future work. Anyway, at present, an insight is that two successive rounds of refinement would narrow the sector \mathfrak{S}_i to much less than one fourth, since it is impossible to split \mathfrak{S}_i nearly even then.

We also notice that the error-bounded quantum search problem is related to the quantum state preparation (QSP) problem, aiming to prepare a user-specified state using basic gates only. The best complexity result at present is $\mathcal{O}(2^n)$ in circuit size (the number of basic gates) and $\mathcal{O}(n + 2^n/(n+m))$ in circuit depth with m ancillary qubits [25, 28]. However, the quantum search admits query operation, can be thought of a QSP problem using the universal gate set $\{G\}$. The exponential hierarchy of such problems is inherent.

Lastly, we would like to study the explicit (closed-form) solution S_{i+1} defined by the recurrent relation in Lemma 5.3. With it a lower bound could be settled for the time complexity of MIP. The bound is conjectured to be $\mathcal{O}(\sqrt{2}^{\|\varepsilon\|})$, as S_{i+1} is approximated by π/θ_i to some extent. Continued fractions [23], we hope, could be a powerful tool to attack it.

Acknowledgements The authors thank the anonymous reviewers whose careful comments improve the presentation significantly, and are also grateful to Profs. Chuanming Zong and Yang Yu for insightful suggestions on the early version of this work.

References

- [1] Ambainis A (2004) Quantum search algorithms. *SIGACT News* 35(2):22–35
- [2] Ambainis A, Bačkurs A, Nahimovs N, Rivosh A (2013) Grover’s algorithm with errors. In: Kučera A, Henzinger TA, Nešetřil J, Vojnar T, Antoš D (eds) *Mathematical and Engineering Methods in Computer Science*, Springer, pp 180–189
- [3] ASRS (2023) Aviation safety reporting system. URL <http://asrs.arc.nasa.gov/>
- [4] Boyer M, Brassard G, Høyer P, Tapp A (1998) Tight bounds on quantum searching. *Fortschritte der Physik* 46(4-5):493–505
- [5] Brassard G, Høyer P, Mosca M, Tapp A (2002) Quantum amplitude amplification and estimation. In: Lomonaco SJ, Brandt HE (eds) *Quantum Computation and Information, Contemporary Mathematics*, vol 305, AMS, pp 53–74
- [6] Chen X, Sun X, Teng SH (2008) Quantum separation of local search and fixed point computation. In: Hu X, Wang J (eds) *Computing and Combinatorics*, Springer, pp 170–179
- [7] Chen YA, Gao XS (2022) Quantum algorithm for Boolean equation solving and quantum algebraic attack on cryptosystems. *Journal of Systems Science and Complexity* 35(1):373–412
- [8] Childs AM, Goldstone J (2004) Spatial search by quantum walk. *Physical Review A* 70(2):article no. 022,314
- [9] Faugère JC, Horan K, Kahrobaei D, Kaplan M, Kashefi E, Perret L (2017) Fast quantum algorithm for solving multivariate quadratic equations. CoRR abs/1712.07211, URL <http://arxiv.org/abs/1712.07211>
- [10] Gong J, Chen Z, Ma C, Xiao Z, Wang H, Tang G, Liu L, Xu S, Long B, Jiang Y (2023) Attention weighted mixture of experts with contrastive learning for personalized ranking in E-commerce. In: Proc. 39th IEEE International Conference on Data Engineering, ICDE 2023, IEEE, pp 3222–3234
- [11] Grover LK (1996) A fast quantum mechanical algorithm for database search. In: Miller GL (ed) Proc. 28th Annual ACM Symposium on the Theory of Computing, ACM, pp 212–219
- [12] Grover LK (2005) Fixed-point quantum search. *Physical Review Letters* 95:article no. 150,501
- [13] Hardy GH, Wright EM (1979) *An Introduction to the Theory of Numbers*, 5th edn. Oxford University Press, London
- [14] Harrow AW, Hassidim A, Lloyd S (2009) Quantum algorithm for linear systems of equations. *Physical Review Letters* 103(15):article no. 150,502
- [15] He X, Sun X, Yang G, Yuan P (2023) Exact quantum query complexity of weight decision problems via Chebyshev polynomials. *Science China Information Sciences* 66(2):article no. 129,503
- [16] Høyer P (2000) On arbitrary phases in quantum amplitude amplification. *Physical Review A* 62(5):article no. 052,304
- [17] Hsieh JY, Li CM (2002) General SU(2) formulation for quantum searching with certainty. *Physical Review A* 65(5):article no. 052,322
- [18] Lehmer DH (1933) A note on trigonometric algebraic numbers. *American Mathematical Monthly* 40(3):165–166
- [19] Li G, Li L (2023) Deterministic quantum search with adjustable parameters: Implementations and applications. *Information and Computation* 292:article no. 105,042
- [20] Long GL (2001) Grover algorithm with zero theoretical failure rate. *Physical Review A* 64(2):article no. 022,307
- [21] McAuley J, Targett C, Shi Q, van den Hengel A (2015) Image-based recommendations on styles

- and substitutes. In: Baeza-Yates R, Lalmas M, Moffat A, Ribeiro-Neto BA (eds) Proc. 38th International ACM SIGIR Conference on Research and Development in Information Retrieval, ACM, pp 43–52
- [22] Nielsen MA, Chuang IL (2000) Quantum Computation and Quantum Information. Cambridge University Press, London
- [23] Olds CD (1963) Continued Fractions. Random House, New York
- [24] Shapira D, Mozes S, Biham O (2003) Effect of unitary noise on Grover’s quantum search algorithm. *Physical Review A* 67(4):article no. 042,301
- [25] Sun X, Tian G, Yang S, Yuan P, Zhang S (2023) Asymptotically optimal circuit depth for quantum state preparation and general unitary synthesis. *IEEE Transactions on Computer-Aided Design of Integrated Circuits and Systems* 42(10):3301–3314
- [26] Tulsi T, Grover LK, Patel A (2006) A new algorithm for fixed point quantum search. *Quantum Information and Computation* 6(6):483–494
- [27] Ye K, Wong KSW, Lim LH (2022) Optimization on flag manifolds. *Mathematical Programming* 194:621–660
- [28] Yuan P, Zhang S (2023) Optimal (controlled) quantum state preparation and improved unitary synthesis by quantum circuits with any number of ancillary qubits. *Quantum* 7:article no. 956